These computations were done by removing the factor "½" in front of the solar-flux term of Eq. 1; this change increased the thermopause temperatures by approximately 50 percent.

18. Private communication with Chamberlain and McElroy indicates that their temperature computations were meant to represent a diurnal and latitudinal planetary average. If, rather, the computations were interpreted as only a diurnal average, they would be applicable to a solar latitude of about 38° on Mars. Thus Chamberlain and McElroy used what corresponds to a daytime mean solar zenith angle of 60°, whereas the average solar zenith angle was about 75° at Electris on the day of the experiment.
19. Below 200 Å we used the quiet-sunspot minimum solar x-ray intensities given in table 4-4 in F. S. Johnson's *Satellite Environment Handbook* (Stanford Univ. Press, ed. 2, 1965) for the sample calculations of Fig. 4. Between 200 and 1000 Å, we used data from H. E. Hinteregger, L. A. Hall, G. Schmedtke, "Solar XUV radiation and neutral particles distribution in July 1963 thermosphere," Intern. Space Sci. Symp. 5th, Florence, Italy, 1964. For longer wavelengths, we used data from fig. 4-2 of F. S. Johnson's *Satellite Environment Handbook*. Chamberlain and McElroy presumably used the data of Hinteregger *et al.* for all wavelengths.
20. S. H. Gross, W. E. McGovern, S. I. Rasool, *Science* **151**, 1216 (1966).
21. A. J. Kliore, D. L. Cain, G. S. Levy, "Radio occultation measurement of the Martian atmosphere over two regions by the Mariner IV space probe," *Seventh International Space Science Symposium*, Committee on Space Research (COSPAR) Vienna, May 1966.
22. R. B. Leighton and B. C. Murray, *Science* **153**, 136 (1966).
23. G. de Vaucouleurs, *Physics of the Planet Mars* (Faber and Faber, London, 1954), p. 202.
24. G. Fjeldbo, V. R. Eshleman, O. K. Garriott, F. L. Smith, III, *J. Geophys. Res.* **70**, 3701 (1965).
25. Research supported by NASA grants NGR-05-020-065 and NsG-377.

10 June 1966 ■

Infrared Analysis of Rat Bone: Age Dependency of Amorphous and Crystalline Mineral Fractions

Abstract. *Quantitative infrared spectrophotometric analysis of whole femurs from male rats demonstrates that amorphous calcium phosphate is a major component of bone mineral. The amount of amorphous calcium phosphate in whole bone decreases while the crystalline bone apatite increases during early stages of bone formation. Mature rat bone contains constant levels of both amorphous and crystalline calcium phosphate.*

In the past, it was thought that the inorganic portion of bone tissue was composed of submicroscopic calcium phosphate crystals which generally resemble the geological mineral hydroxyapatite, but recent studies indicate that this conceptually simple, one-compartment model of bone mineral is actually an oversimplification of the physical state of the tissue (*1*). X-ray diffraction studies of bone show that the mineral fraction is composed of two separate phases, amorphous (noncrystalline) calcium phosphate and crystalline apatite (*1*). This report presents evidence, based on infrared spectrophotometric analysis, for the two-phased nature of bone mineral which indicates that the amorphous and crystalline calcium phosphate fractions of whole rat bone are interrelated. The significance of this finding not only applies to bone structure and metabolism but also affects the interpretation of many observed physical and chemical properties of bone. The net properties of bone mineral must now be considered as variable averages of the individual properties of its two calcium phosphate constituents (*2*).

The triply degenerate, antisymmetric bending vibration of the orthophosphate ion absorbs infrared radiation at wave numbers between 500 and 600 cm^{-1} for both amorphous calcium phosphate and crystalline apatite. Amorphous calcium phosphate gives a broad and symmetrical single absorption band in this region, while the anisotropic local electric field of crystalline apatite partially splits the degeneracy of this absorption band into a well-defined doublet (*3*). A third band at 630 cm^{-1}, arising from first order hydroxide ion librational (hindered rotational) motion, is found as a shoulder on this 600 cm^{-1} phosphate band only in large synthetic hydroxyapatite crystals (*3*).

Mixtures of amorphous calcium phosphate and crystalline apatite exhibit varying degrees of splitting for the phosphate ion antisymmetric bending mode, depending upon their weight fractions within the mixture (*3*). We found a straight line correlation between the degree of this infrared splitting and percentage crystallinity (weight fraction of crystalline apatite) in synthetic samples containing these two phases (*4*). The method used for determining this splitting quantitatively is shown in Fig. 1. A connecting line is constructed between the points of minimum transmission for the two peaks, marking off the area A_1. A best base line is then drawn from 450 cm^{-1} to 700 cm^{-1} at the top of the absorption band, marking off the area A_2. Since none of the spectra examined in this study contained a hydroxide ion shoulder at 630 cm^{-1}, A_2 always represented only phosphate ion absorption. The areas A_1 and A_2 were measured with the aid of a planimeter, affording relative standard deviations of ± 3 percent. The ratio of A_1 to A_2, which we call the splitting fraction (SF), measures the amount of splitting for any given sample with a relative standard deviation of ± 4 percent.

All spectra were recorded on a Beckman IR-12 infrared spectrophotometer under double beam conditions using the instrument's standard mechanical slit program with a frequency drive speed of 40 cm^{-1} per minute and a strip chart recorder expansion rate of 50 cm^{-1} per inch (2.5 cm). In each case, total absorption was adjusted so that transmission was between 85 and 90 percent at the base line. Only those spectra that gave a minimum transmission of 45 to 50 percent as measured at the midpoint of the absorption band (base line to constructed line) were used for SF analysis.

As mentioned previously, this method was applied to the determination of percentage crystallinity in well-defined synthetic calcium phosphate samples (*4*). However, in order to extend the method to bone tissue, a number of pertinent parameters must be taken into account. These are particle size, sample concentration and path length, extraneous compounds, crystal size and stoichiometry, and protein content.

For infrared analysis our samples were mixed with potassium bromide in the following way. All samples were sieved on 250- to 300-mesh screens after they had been ground in a Spex grinder, and the mineral content of each bone sample was predetermined by a measurement of ash weight, so that we could add an original sample weight containing 2.0 ± 0.1 mg of mineral to 700 ± 1 mg of KBr matrix. The sample and matrix were then blended in a Spex grinder and made into pellets, each being pressed under vacuum in a circular die, 22 mm in diameter, under 30 tons ram force in a Limit 30-ton pellet press (approximately 6000 atm). Thus, particle size and sample-matrix homogeneity can be kept constant, and transparent pellets with reproducible mineral concentrations and path lengths can be obtained.

We found no change in SF values

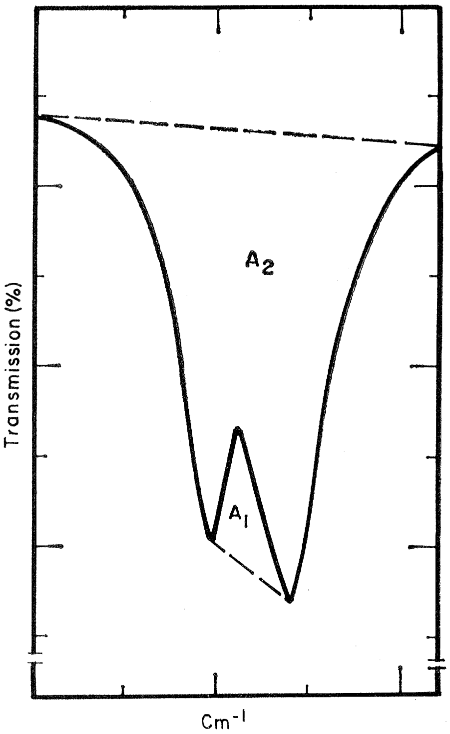

Fig. 1. Splitting fraction measurement for the 600 cm^{-1} phosphate ion antisymmetric bending frequency in the calcium phosphates.

after adding as much as 20 percent by weight of heparin sulfate, β-glycerol phosphate, glucose-6-phosphate, sodium citrate, or calcium carbonate to synthetic calcium phosphates. Carbonatoapatites were excluded from this investigation, since the sizes of their crystals (*5*) are outside the size range of apatite in rat bone (*6*). Precipitates of small-sized crystalline apatites containing large amounts of carbonate were also excluded, since it has been shown that these salts contain an appreciable amount of amorphous calcium phosphate (*7*). Finally, the absorption spectra obtained from 10- and 150-day-old rat bone, demineralized with ethylenediaminetetraacetate (EDTA), indicate that there are no bone protein absorption bands in the SF region.

We found no difference in SF values for apatites of the same crystal size but with different Ca/P molar ratios. We also found that the variation in SF produced by fully crystalline apatites, with varying sizes of crystals within the size range of rat bone apatite (*6*), was random and within the error of the measurement. However, apatites with crystal sizes much larger than rat bone apatite had slightly higher SF values. Adding EDTA-demineralized bone protein to synthetic calcium phosphates decreases the SF values, but the amount of protein added (beyond a minimum amount) is not a critical factor. For example, the deviation in SF values obtained from mixtures of synthetic calcium phosphates and demineralized bone protein (added protein ranging from 15 to 80 percent) was random and within the error of the method.

Based on these observations, standard regression lines (Fig. 2) for analysis of percentage crystallinity by SF measurement can be constructed. The dashed line is a plot of SF versus percentage crystallinity for a series of mixtures of synthetic amorphous and apatitic calcium phosphates. The solid line, used for the analysis of bone, is the standard regression line for a series of synthetic bone mock-ups of different crystallinity percentages which were homogeneous mixtures of synthetic calcium phosphates and powdered bone protein, the range of protein being 15 to 80 percent. Both lines were constructed from points that are the average of ten separate measurements. This method affords a ± 5 percent error in values for percentage crystallinities.

Femurs were obtained immediately after male Wistar rats, ranging from 8 to 264 days old, were killed. After dissection, the bones were quick-frozen in a bath of dry ice and alcohol and ground to 50 mesh with powdered dry ice in a Wiley mill. The frozen bone powders were then lyophilized and subsequently ground to 250 mesh in a Spex grinder. These bone samples were prepared for infrared analysis by the methods described above and the results (averages of triplicate analyses) are given in Table 1. As a check, the percentage crystallinity values of the 13-, 18-, 29-, and 38-day-old femurs were also measured by x-ray diffraction (*1*). Values obtained by this method were found to be within ± 2 percent of the results obtained for these bones by infrared analysis.

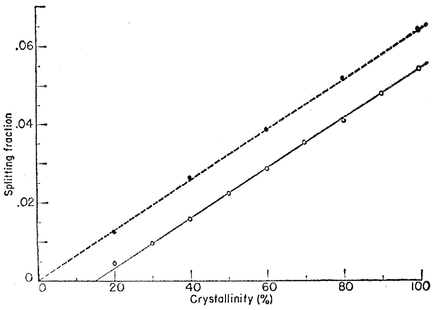

Fig. 2. Standard regression lines for infrared spectrophotometric percent crystallinity analysis. Open circles, bone mock-up; closed circles, no protein added.

Young bone contains much more calcium phosphate in the amorphous than in the crystalline apatite state (Table 1). As bone grows this is gradually reversed until, at maturity, there is a constant level of both phases of calcium phosphate in a ratio of crystalline to amorphous of approximately 2 : 1. This age-dependent change in percentage crystallinity implies an interrelation between the two phases of calcium phosphate in growing intact bone. Changes observed for entire limbs may arise from alterations in the relative masses of epiphyseal, metaphyseal, and diaphyseal tissue concomitant with growth. For example, the 8-day-old rat femur contains large amounts of cartilaginous as well as bony tissue, while the 264-day-old rat femur is mostly compact bone. Any difference in the amorphous-crystalline mineral compositions of the various bone and cartilage

Table 1. Analysis of percentage crystallinity of rat bone by infrared spectrophotometric splitting fraction (SF) measurement.

Age of rat femurs (days)	Ash (%)	Ca/P molar ratio	SF	Mineral content (%)	
				Amorphous	Crystalline
8	18.4	1.41	0.0100	69.5	30.5
13	30.0	1.46	.0185	56.0	44.0
18	32.3	1.50	.0240	47.0	53.0
29	44.3	1.55	.0300	37.5	62.5
32	42.1	1.55	.0305	37.0	63.0
35	44.8	1.57	.0315	35.5	64.5
38	43.8	1.56	.0310	36.0	64.0
41	46.5	1.59	.0310	36.0	64.0
44	44.7	1.58	.0310	36.0	64.0
47	46.9	1.59	.0315	35.5	64.5
50	47.8	1.60	.0310	36.0	64.0
53	47.1	1.60	.0310	36.0	64.0
56	50.1	1.61	.0315	35.5	64.5
264	56.6	1.63	.0315	35.5	64.5

tissue regions representing different stages of bone formation would result in different overall mineral compositions for the entire limb. Therefore, it must be realized that the percentage crystallinity value given for a whole limb represents an average assay of the mineral in a mixture of tissues comprising that limb.

The fact that young bone contains much more amorphous than crystalline mineral suggests that amorphous calcium phosphate may be the first mineral deposited during the overall process of bone formation. As a verification of this, we found, by x-ray diffraction analysis of chick bones, that mineral in the epiphyseal tissue is only 20 percent crystalline (80 percent amorphous), while in the metaphyseal tissue mineral is 60 percent crystalline and 40 percent amorphous (*8*).

The value for nonhaversian, 264-day-old compact rat bone mineral is identical with that obtained for haversian cortical cow bone by infrared analysis, which seems to indicate that amorphous calcium phosphate is present in all bone tissue, independent of microanatomical considerations. This is not surprising since, on a molecular level, amorphous calcium phosphate is a precursor of crystalline apatite in synthetic systems (*9*). These facts are consistent with evidence obtained by electron microscopy which indicates that a noncrystalline mineral phase appears prior to crystalline apatite during early stages of bone formation (*10*). Thus, it may be true that amorphous calcium phosphate can act as a metabolic precursor of crystalline apatite in bone.

We also analyzed surgically separated, adult human dentine and enamel. Enamel samples were 100 percent crystalline apatite, while the mineral portion of the dentine was 65 to 70 percent crystalline. Thus, dentine has a mineral composition akin to that of compact bone, while the much harder and more chemically inert dental enamel consists of only crystalline apatite.

The presence of amorphous calcium phosphate in hard tissues is an important parameter that must be considered in any discussion of the properties of these tissues. For example, there may actually be two separate and distinct mineral ion metabolic pools in skeletal tissue. Moreover, amorphous calcium phosphate may be the first mineral deposited during the calcification process and may subsequently act as a metabolic precursor of crystalline apatite in calcified tissues. The two-phased nature of bone mineral may prove to be a valuable aid in understanding the operative mechanisms of bone metabolism and the molecular basis of bone structure.

JOHN D. TERMINE
AARON S. POSNER

Hospital for Special Surgery,
Cornell University Medical College,
New York, New York 10021

References and Notes

1. J. D. Termine, thesis, Cornell University, 1966; R. A. Harper and A. S. Posner, *Proc. Soc. Exp. Biol. Med.* **122**, 137 (1966).
2. J. A. Prins, in *Physics of Non-Crystalline Solids*, J. A. Prins, Ed. [Interscience (Wiley), New York, 1965], p. 1.
3. J. M. Stutman, J. D. Termine, A. S. Posner, *Trans. N.Y. Acad. Sci.* **27** (1965), 669 (1965).
4. J. D. Termine and A. S. Posner, *Nature* **211**, 268 (1966).
5. R. Zapanta-LeGeros, *Nature* **206**, 403 (1965).
6. A. S. Posner, R. A. Harper, S. A. Muller, J. Menczel, *Ann. N.Y. Acad. Sci.* **131**, 737 (1965).
7. B. N. Bachra, O. R. Trautz, S. L. Simon, *Arch. Biochem. Biophys.* **103**, 124 (1963).
8. J. D. Termine and A. S. Posner, in preparation.
9. E. D. Eanes, I. H. Gillessen, A. S. Posner, *Nature* **208**, 365 (1965); E. D. Eanes and A. S. Posner, *Trans. N.Y. Acad. Sci.* **28**, 233 (1965).
10. R. A. Robinson and M. L. Watson, *Ann. N.Y. Acad. Sci.* **60**, 596 (1955); S. Fitton-Jackson and J. T. Randall, in *Bone Structure and Metabolism*, G. E. W. Wolstenholme and C. M. O'Conner, Eds. (Churchill, London, 1956), p. 47; Z. Molnar, *J. Ultrastruct. Res.* **3**, 39 (1959); H. J. Höhling, H. Theman, J. Vahl, in *3rd European Symposium on Calcified Tissues*, H. Fleisch, H. J. J. Blackwood, M. Owen, Eds. (Springer-Verlag, Berlin, 1966), p. 146.
11. Supported in part by grant No. DE-01945 from the National Institute of Dental Research.

10 June 1966

Electrical Resistivity Changes in Saturated Rock under Stress

Abstract. *Electrical resistivity of water-saturated crystalline rock such as granite, diabase, dunite, or quartzite changes by an order of magnitude prior to fracture of the rock in compression. The effect observed even under high confining pressure is due to formation of open cracks which first appear at one-third to two-thirds the fracture stress.*

Fracture of brittle materials usually occurs without much warning. If a rock such as granite is stressed in compression, for example, there is little in the stress-strain curve preceding fracture which might predict the point of fracture. However, a number of subtle changes in the structure of the granite do occur prior to fracture. These changes, although not apparent in the axial stress-strain curve, exert a marked influence on certain properties. The most striking effect observed is on the electrical properties; electrical resistivity changes by an order of magnitude prior to fracture of water-saturated crystalline rocks.

Two observations suggested that large changes in resistivity might precede the fracture of rock. Sensitive measurements of volume change (*1*) showed that many rocks became dilatant, that is, they increased in volume slightly, as they were deformed in compression. Surprisingly, this was observed even when specimens were deformed at a confining pressure of 8 kb. The amount of volume increase, relative to elastic changes, was small; typically, it was of the order of a few tenths of a percent. Nevertheless, increase in volume could be detected at one-third to two-thirds the fracture stress. The increase in volume was traced to new cracks which were apparently open and which were strongly aligned parallel with the direction of maximum compression.

Conduction of electricity (through cracks and pore spaces) in a water-saturated crystalline rock such as dunite or granite is primarily ionic. In the laboratory samples the effect of hydrostatic pressure on conductivity is striking (*2*) because of the way in which cracks and pores change shape under pressure. An increase in confining pressure of 10 kb changes resistivity of common crystalline rocks by as much as three orders of magnitude (Fig. 1). A large percentage of this change occurs in the first 2 kb; measurements of linear compressibility and other elastic parameters in this range (*3*) suggest the reason. Most rocks such as granite have minute porosity in the form of cracks; these cracks are closed by a pressure of a few kilobars. The remaining pore spaces are more equant in shape so that further changes in the cross section of conduction paths take place much more slowly as pressure is raised.

When combined, these two sets of observations suggest that if a saturated rock is stressed in compression, one might first see resistivity increase (preexisting cracks forced shut) and then, at about one-third to two-thirds the fracture stress, see rapid decrease (rock becomes dilatant and new cracks form). To observe this effect one would have to ensure that water could move freely in and out of the rock, so that potential conduction paths would contain water.

We measured the effects of stress